A direct method to produce and measure compositional grading in AlxGa1−xAs alloys

M. Sundaram, Achim Wixforth, R. S. Geels, A. C. Gossard, J. H. English

Angaben zur Veröffentlichung / Publication details:

Sundaram, M., Achim Wixforth, R. S. Geels, A. C. Gossard, and J. H. English. 1991. "A direct method to produce and measure compositional grading in AlxGa1−xAs alloys." *Journal of Vacuum Science and Technology B: Microelectronics and Nanometer Structures* 9 (3): 1524–29. https://doi.org/10.1116/1.585460.

A direct method to produce and measure compositional grading in $Al_xGa_{1-x}As$ alloys

M. Sundaram, A. Wixforth, R. S. Geels, et al.

Citation: Journal of Vacuum Science & Technology B: Microelectronics and Nanometer Structures Processing, Measurement, and Phenomena **9**, 1524 (1991); doi: 10.1116/1.585460

View online: https://doi.org/10.1116/1.585460

View Table of Contents: https://avs.scitation.org/toc/jvn/9/3

Published by the American Institute of Physics

A direct method to produce and measure compositional grading in $Al_xGa_{1-x}As$ alloys

M. Sundaram, A. Wixforth, R. S. Geels, A. C. Gossard, and J. H. English
Department of Electrical Engineering, and Materials Department, University of California, Santa Barbara, California 93106

(Received 3 December 1990; accepted 31 January 1991)

We present a method to calibrate the profile of Al mole fraction versus depth, deposited in growth of graded $Al_xGa_{1-x}As$ alloys in a molecular-beam epitaxy machine. A computer is used to either ramp the Al oven temperature (analog alloy), or pulse the Al beam (digital alloy), with a fractional monolayer depth resolution that permits averaged alloy profiles corresponding to a range of different design profiles to be obtained. The profiles are measured in calibration runs by using a fast picoammeter to track the ion-collector current of the beam flux monitor ion gauge (facing the ovens), and integrating the ion current with time. Parabolic quantum wells are grown by either technique and the corresponding measured profiles are compared to each other and to the design profile. The ability of the digital-alloy technique to obtain almost arbitrarily varying graded-alloy profiles is illustrated.

I. INTRODUCTION

Tailoring of the energy band gap in semiconductor heterostructures is a useful technique of controlling the electronic and optical properties of carriers in devices made from these materials. Examples are the single (multi) quantum well *p-i-n* laser in which the intrinsic region consists of a square well(s) with parabolically graded barriers (e.g., the GRINSCH laser),[1] and heterojunction bipolar transistors (HBTs) with graded-gap base regions.[2] The scope of this technique is so wide that it is referred to generally as band gap engineering.[3] Modern epitaxial growth techniques such as molecular-beam epitaxy (MBE) lend themselves readily to the growth of abrupt or smoothly graded $GaAs/Al_xGa_{1-x}As$ heterointerfaces.[4]

Recently, a series of structures have been devised in which modulation doping and a graded band gap have been combined to obtain a high-mobility electron gas with a controlled static density distribution.[5] In the structures which were studied, electrons were introduced into wide parabolic wells by remotely doping the barrier layers surrounding the well. The parabolic potential wells were themselves created by appropriately grading the mole fraction x of an $Al_xGa_{1-x}As$ alloy layer. The electrons were found to distribute themselves across the parabolic well with the density being governed by the curvature of the design parabola, in the limit of absolute zero of temperature. These high-mobility uniform electron gases or three-dimensional electron gas (3DEGs) are the best experimental approximation to the theoretical construct of jellium, and have exhibited a number of interesting properties in transport measurements.[6,7] Grading of the band gap allows a wide range of densities to be achieved. Modulation doping results in high carrier mobilities of these gases without low temperature carrier freeze-out.

These and other graded structures are often realized in the $GaAs/Al_xGa_{1-x}As$ system, where there exists a nearly linear relationship between the $Al_xGa_{1-x}As$ energy band gap and Al mole fraction x for $x < 0.45$.[8] Controlled variation of x results in a corresponding controlled variation of the alloy band gap. The variation of x with depth in a thin film can itself be achieved in two ways. The Al flux can be changed during growth in a controlled manner by controlling the temperature of the Al oven in an MBE machine, in the presence of constant Ga and As fluxes.[9] We refer to the alloy obtained in this way as an analog alloy. One could alternately grow a superlattice with a constant period (sufficiently small to permit tunneling of electrons between the layers), each period being composed of two layers: GaAs and $Al_yGa_{1-y}As$, where y is greater than or equal to the maximum Al mole fraction in the graded alloy. The duty cycle of the $Al_yGa_{1-y}As$ is varied in a controlled manner so that the average Al mole fraction follows the desired profile.[10] In other words, the Al beam is pulsed in controlled fashion by controlling the Al oven shutter in an MBE machine. We refer to the alloy obtained by the latter technique as a digital alloy.

The actual profile of Al mole fraction versus depth obtained is not easily measured directly. Its general shape is sometimes deduced from optical or electrical measurements on the resulting structures,[11] followed by a fitting of the data to calculations for the designed energy bandgap profile. These techniques are indirect at best. Techniques like secondary ion mass spectrometry (SIMS) have limited depth resolution, and are destructive besides.

In the present work we present a method to calibrate deposited Al mole fraction versus depth before growth with a simple, reproducible technique having reasonably high resolution and accuracy. The measurement is done in the MBE machine itself in a calibration run immediately prior to sample growth. If the variation from one measured run to another is negligibly small, the measured profile can be reasonably assumed to be the actual profile grown.

The Al flux can be measured by a beam flux monitor that consists of an ion gauge (Bayard–Alpert gauge in a Varian GEN II MBE system). The beam flux monitor gauge that is

 0734-211X/91/031524-06$01.00

used for this purpose can be made to directly face the ovens. The collector current (usually in the range of nA) of the ion gauge is fed to a fast picoammeter. The variation of Al flux $F_{Al}(t)$ with time is therefore measured directly. Inasmuch as actual growth occurs in the presence of a constant Ga flux, a constant collector current corresponding to the Ga flux F_{Ga} is assumed in the calculations. F_{Ga} is adjusted to be in the same ratio to a particular F_{Al}, say F_{Al} $(t=0)$, as the ratio of the corresponding GaAs and AlAs growth rates, which are in turn determined by reflection-electron-diffraction (RED) oscillations[12] immediately prior to the ion-gauge measurement. Integrating the total flux F_{total} ($F_{total} = F_{Al} + F_{Ga}$) from time $t=0$ until time $t=T$:

$$z = \int_0^T F_{total}(t)dt, \tag{1}$$

gives us a measure of the thickness z of the graded alloy grown until time T. Integrating $F_{Al}(t)$ and $F_{total}(t)$ over a time interval ΔT centered at T, gives the Al mole fraction $x(z)$ as

$$x(z) = \left(\int^{\Delta T} F_{Al}(t)dt \Big/ \left\{\int^{\Delta T} [F_{Al}(t) + F_{Ga}]dt\right\}\right). \tag{2}$$

The variation of Al mole fraction x with depth z can therefore be measured and compared with the design profile.

The method is applicable to measuring the alloy grades of both analog and digital alloys. The Al fraction in the alloy may in places be designed to be very small. In the digital alloy technique this requires very rapid pulsing of the pneumatic shutter of the Al oven and thence of the Al beam. This causes corresponding rapid changes in the collector current of the ion gauge. Hence the need for a fast picoammeter to track the current.

II. EXPERIMENTS AND DISCUSSION

Measurements were made in a Varian Gen II MBE machine used for the growth of GaAs/$Al_xGa_{1-x}As$ epilayers. Oven temperatures and shutter opening times are controlled by a HP-9000 Series 300 instrument controller having a time resolution of 10ms. The equation of the desired alloy profile versus depth is used by the computer program to generate a ramp of Al oven temperature with time (analog alloy), or a sequence of shuttering times of the Al oven pneumatic shutter (digital alloy), with a resolution fine enough to produce a smooth alloy gradient. The ion gauge of the beam flux monitor faces the ovens, and is situated at the same location where the substrate would be during actual growth. The collector current of the beam flux monitor is measured with a Keithley 480 picoammeter. The analog output of the picoammeter is fed back to the controller via a fast analog–digital converter. All computations are then performed by the controller at the end of the run.

Figure 1 shows measured profiles of Al flux $F_{Al}(t)$ with time, for a single pulse 0.5 s long (the command to open being issued at time $t=0$, and the command to close being issued at time $t=0.5$ s). The profiles correspond to measurements of the same pulse, with two different rise time settings (7 and 70 ms, respectively), corresponding to two different sensitivity scales of the picoammeter. The 70 ms

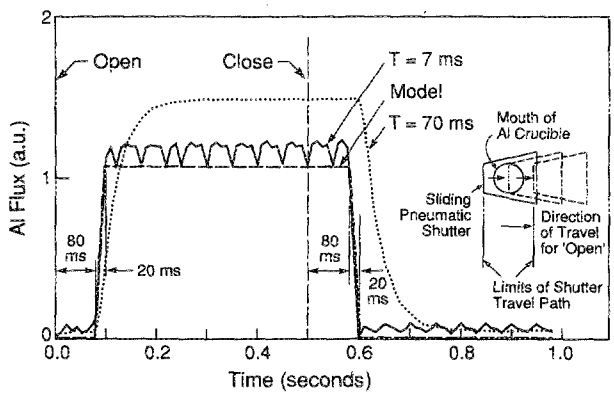

FIG. 1. Beam flux monitor (BFM) ion gauge measured flux profiles of 0.5 s Al pulse in an MBE machine: solid profile for a range having a 7 ms rise time, dotted profile for 70 ms rise time. The "open" command is issued to the pneumatic shutter at time $t=0$, and the "close" command at $t=0.5$ s. Opening and closing delays of ~80 ms, and ramp-up and ramp-down times of ~20 ms are measured. The assumed ideal flux profile (dashed) is also shown. Inset shows the finite speed at which the shutter slides across the crucible mouth as the origin of these delays. The semiperiodic interference spikes in the solid trace occur whenever the picoammeter is used to measure the ion-collector current with a fast response time setting.

response time is seen to dominate the rise and fall times of the dashed profile. The shorter response time setting of 7 ms is needed to resolve the speed of rise and fall of the actual profile, as seen by the solid line. A nearly periodic background interference signal is seen in the solid profile due to the fast rise time setting of the picoammeter. Note the opening and closing delays, and the finite times to ramp up the flux and to ramp it down. The inset shows the origin of these delays. The pneumatic shutter travels for a finite distance on either side of the crucible mouth, giving rise to the open (T_{open}) and close (T_{close}) delays. Besides motion time, electronic delay, and shutter backlash also contribute to the open and close delays. The travel across the face of the Al crucible itself gives rise to the ramp-up and ramp-down times. Inasmuch as all other times involved in the measurement: ion collection time in the gauge's electric field, picoammeter and A–D converter delays, are smaller than the 10 ms clock resolution of the computer, the measured solid profile of Fig. 1 is believed to reflect the true delays of the pneumatic shutter. The open (T_{open}) and close (T_{close}) delays are thus of the order of 80 ms and both the ramping times ($T_{ramp\ up}$ and $T_{ramp\ down}$), of the order of 20 ms. The true profile is approximated by a trapezoidal profile with all these time constants incorporated (also shown in Fig. 1). The actual time that the Al oven shutter is to be opened for a given thickness of AlAs to be grown in, say, a superlattice, is automatically computed in the program taking these delays into consideration.

There are three possible scenarios for a shutter opening and closing sequence. Case 1, outlined in Fig. 1, is where the shutter moves all the way across the face of the oven and comes to rest at the other end of travel, before receiving a command to close. Case 2 is where the shutter uncovers the crucible completely, but is asked to return before it can reach the end of its travel. Case 3 is where the shutter only partially uncovers the oven, before starting on its return path.

Cases 2 and 3 are illustrated in Fig. 2. The measured flux

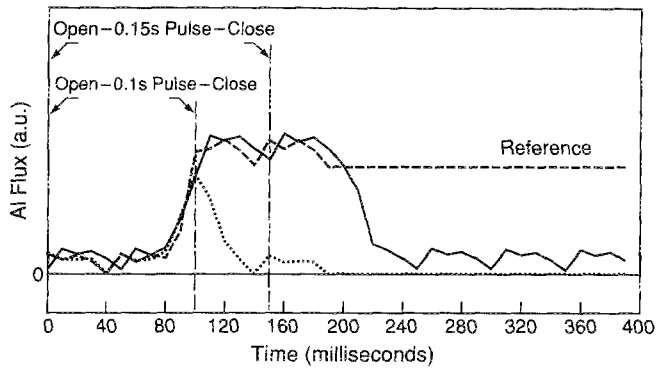

FIG. 2. Ion gauge measured flux profiles of 100 ms (dotted) and 150 ms (solid) Al pulses. In both cases, the pulse is so short that the shutter does not come to rest at the end of its travel after uncovering the crucible. It receives a command to reverse direction and close the oven, before reaching the end of its open path (regime 2). The 100 ms pulse is so short that it only partially uncovers the crucible (regime 3). The flux profile of a longer 0.5 s (dashed) (regime 1) pulse is also shown for reference. The flux profiles have the same time constants as in Fig. 1 and can be modeled as truncated trapezia of the model in Fig. 1.

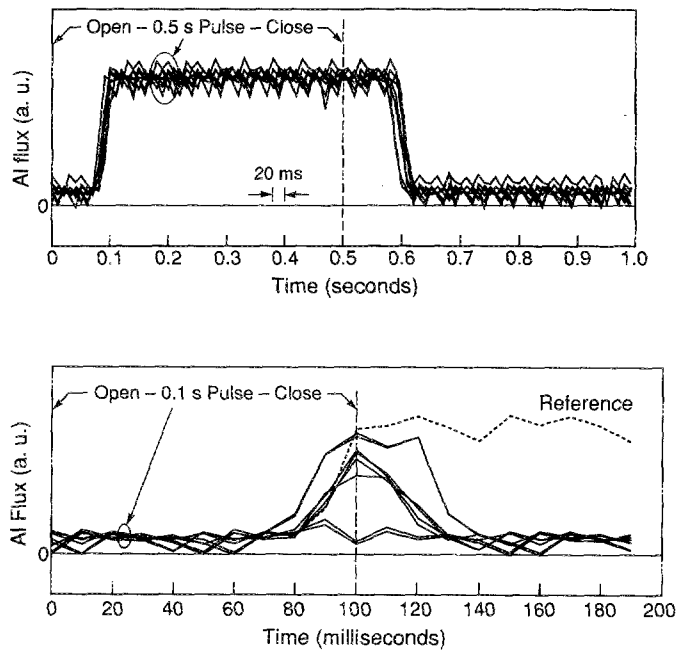

FIG. 3. Jitter in time constants observable in flux profiles of eight consecutive and independent Al pulses of 0.5 s (3a) and 0.1 s (3b) durations. The jitter is $\sim \pm 10$ ms for the longer pulse (regime 1), and ± 20 ms for the sharp pulses of the shutter operating in regimes 2 and 3.

profiles can reasonably be approximated by truncated trapezia with the same time constants as measured for case 1, and are used to deduce Al oven shutter open times for the correct integrated flux for extremely rapid Al pulses.

The three cases occur when the following relationships are satisfied between the four shutter time constants, the AlAs growth rate R_{AlAs}, and the AlAs layer thickness L_{AlAs} grown:

$$\textit{case 1:}\quad \frac{L_{AlAs}}{R_{AlAs}} \geqslant T_{12} \equiv \frac{T_{\text{ramp up}} + T_{\text{ramp down}}}{2} + 2T_{\text{close}}, \tag{3a}$$

$$\textit{case 2:}\quad T_{12} \geqslant \frac{L_{AlAs}}{R_{AlAs}} \geqslant T_{23} \equiv \frac{T_{\text{ramp up}} + T_{\text{ramp down}}}{2}, \tag{3b}$$

$$\textit{case 3:}\quad \frac{L_{AlAs}}{R_{AlAs}} \leqslant T_{23}. \tag{3c}$$

The mechanical inertia and free play of the pneumatic shutter, and the 60 Hz phase difference with respect to the trigger pulse, is expected to cause a certain amount of time jitter in the edges of the flux profile. This jitter is estimated to be of the order of $\Delta T_J \sim \pm 10$ ms for case 1 in Fig. 3(a), where the Al oven shutter is opened for $T = 0.5$ s in eight sequential and independent runs. The uncertainty in the thickness of AlAs grown is therefore of the order $\sim \Delta T_J R_{AlAs}$ (where, R_{AlAs} = growth rate of AlAs). Even for a growth rate of AlAs as high as 1 μm/h, this is negligibly small ($\sim$0.03 Å). The jitter is expected to be more pronounced for cases 2 and 3, as the forward motion of the shutter is arrested and its direction of travel reversed. This is indeed seen to be the case in Fig. 3(b) where in eight independent runs for a fast Al pulse (case 3), the shutter does not uncover the crucible mouth some of the time. The uncertainty in the Al flux deposited is $\pm$ 0.06 Å in this case, for R_{AlAs} = 1 μm/h. This error in the Al mole fraction can be reduced by simply going to lower GaAs and AlAs growth rates. Having a nonzero Al mole fraction minimum in the alloy so that one is always operating in the case 1 regime can also reduce this error. The nonzero minimum Al mole fraction is also desirable in an analog alloy in order to keep the Al oven temperature at levels where the growth rate vs oven temperature follows the behavior deduced from RED oscillations for higher oven temperatures.

The growths of two parabolic wells, one analog and the other digital, both 2000 Å wide and with the Al mole fraction going from 0.01 (1%) at the center of the well to 0.3 (30%) at the well edges, was then run, and the corresponding ion-gauge profiles are compared to the ideal design profile in the top half of Fig. 4. The deviations Δx_{Al}, from the ideal profile are plotted in the bottom half, and are seen to be <0.02 in the case of the digital alloy and <0.03 for the analog alloy. The maximum Al oven temperature in either case was one that gave an AlAs growth rate of 0.32 μm/h. A 1% minimum Al mole fraction at the well center ensured that the shutters were operating in the case 1 regime even at the well center for the digital alloy, and the Al oven temperature changed through no more than 200 °C for the analog alloy. The superlattice period was 20 Å for the digital alloy; for the analog alloy, the temperature of the Al oven was changed at a variable rate, each time interval corresponding to the time required to grow 20 Å of alloy material at the particular Al oven temperature. The Al flux is measured every 10 ms and integrated so that the average Al mole fraction is plotted with the same resolution as the period, in this case 20 Å. The picoammeter noise when integrated, has a nonzero value and consequently produces a constant offset in the measured graded profile. This offset is small (usually $<1\%$ Al) and measurable in a simple run in which the Al oven is not opened at all. This is then subtracted from the measured profile to obtain the corrected profile.

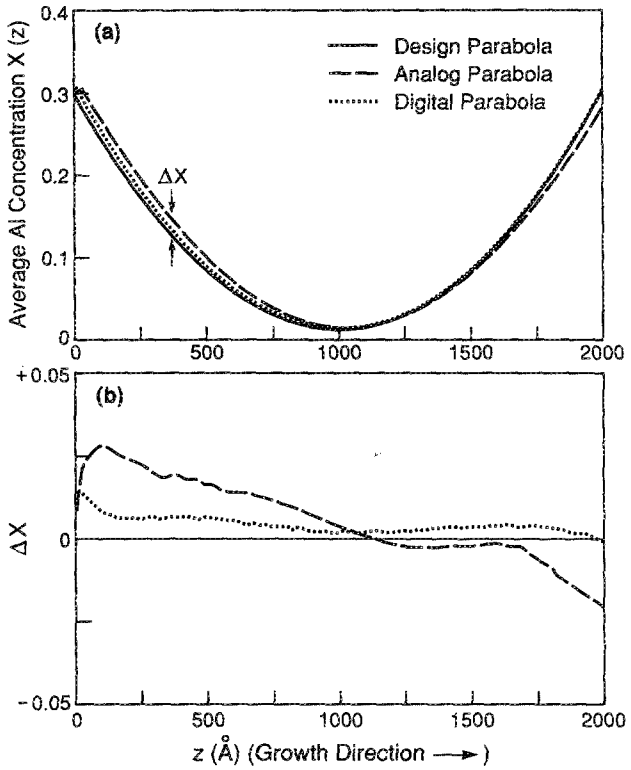

FIG. 4. Measured Al mole fraction (mf) vs depth profiles for a 2000 Å wide parabolic well with Al mf going from 1% at the center to 30% at the edges, grown with both the pulsed Al beam (digital alloy), and the variable Al oven temperature (analog alloy) methods. The design profile is also shown for comparison. A constant background GaAs growth rate of 0.75 μm/h is assumed. Bottom half shows deviations of both measured alloy grades from design alloy.

The shift of the analog profile from the ideal profile observed is a result of the limits of cooling and heating rates of the Al charge. The Al charge is cooled simply by thermal conduction and radiation and has therefore a certain maximum cooling rate. Sufficient controllability of the negative gradient of Al mole fraction versus time is still possible even with a high constant background GaAs growth rate of 0.75 μm/h, as manifested by the measured analog-alloy parabolic well.

To accentuate the differences between the ability of the two alloy techniques to follow a desired profile, a $(\mathrm{Sin}\, z)/z$-type alloy grade profile, spread over a width of 2000 Å, and with maximum and minimum Al mole fractions of 30% and 1%, respectively, was generated. The ion gauge measured profiles are shown along with the design profile in Fig. 5. Note the considerably greater ability of the digital-alloy technique to obtain the desired alloy profile. While the analog-alloy profile does satisfy the required functional behavior, it has smaller amplitude and is broadened. One could, in principle, grow the analog alloy infinitesimally slowly so that the Al oven temperature could be changed in a more controlled manner, but this has the disadvantages of both longer growth times and possibly greater incorporation of background impurities in the growing alloy. It would also be possible to compensate for the time of oven response in the analog alloy growth by modifications in the temperature program as in Ref. 9.

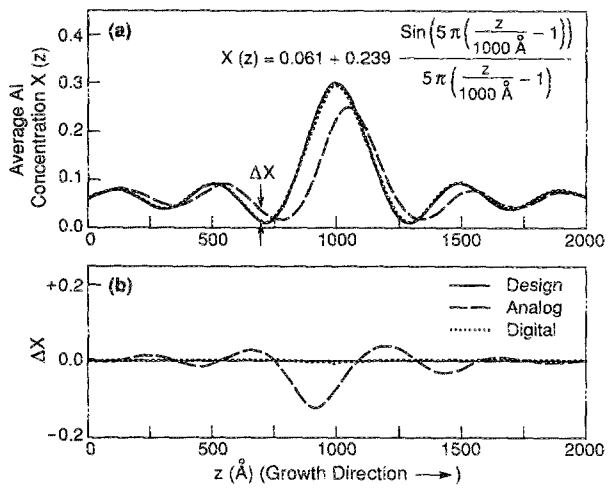

FIG. 5. $(\mathrm{Sin}\, z)/z$-type alloy grade spread over 2000 Å and with minimum and maximum Al mf s of 1% and 30%, measured for both analog and digital alloys. Note greater ability of digital alloy to produce desired profile, and the thermal lag problem in analog-alloy growth.

There is no necessity to have a nonzero minimum Al mole fraction in the alloy, especially in the digital-alloy technique. For usual AlAs growth rates, the Al mole fraction when the shutter is pulsed in the regimes of cases 2 and 3 above, is so small that deviations in the same are scarcely observable. This can be seen in the digital-alloy ion gauge measured profiles of Fig. 6, where the design alloy is a parabolic well 2000 Å wide with Al mole fraction going from 0% at the center to 30% at the edges. Five sequential and independent runs of the same design are shown, along with the ideal profile. Deviations from the design parabola are less than $\Delta x_{\mathrm{Al}} \sim 0.03$. The largest portion of the deviation comes, in fact, from the AlAs growth rate being higher than the design value, and not from any shutter-timing-related uncertainties. The variation from run to run is also observed to be sufficiently small to permit one to predict the actual Al mole fraction versus depth grown, from an ion-gauge profile measured in a dummy run immediately prior to actual growth, to within $\Delta x_{\mathrm{Al}} \sim \pm 0.01$.

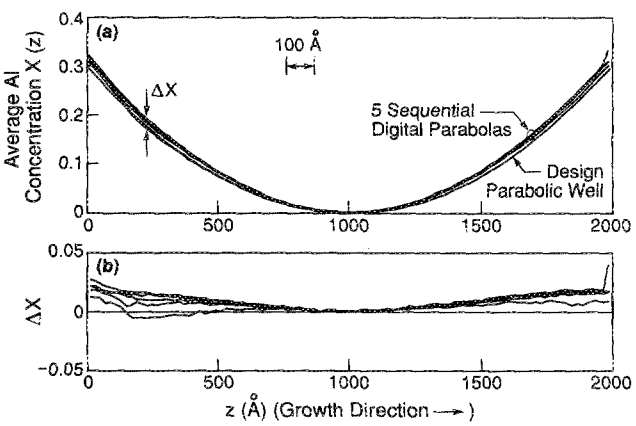

FIG. 6. Alloy profiles of five consecutive and independent digital-alloy parabolic wells, 2000 Å wide and with Al mf rising from 0% at well center to 30% at well edges, measured by ion-gauge method. Variations from run to run are small enough that a measurement made prior to actual sample growth can be taken to represent the actual graded-alloy grown.

For electron gases in wide parabolic potential wells the design parameter of interest is the well curvature, inasmuch as the carrier density profile is controlled by it. Curvature versus depth profiles calculated from the digital and analog alloy profiles measured in Fig. 4, are shown in Fig. 7 and compared to the constant design curvature. A part of the observed variation in curvature ($\sim \pm 11\%$) for the digital alloy arises from the ± 10 ms jitter in the opening and closing times of the shutter operating in regime 1. Should the Al mole fraction go to zero at the well center, the larger uncertainty in the time constants of the shutter operating in regimes 2 and 3 will cause larger (up to $\pm 100\%$) variations in the curvature. In such measurements a flat spot is sometimes observed to occur at the well center with the curvature going to zero.

If one desires to avoid the large percentage errors in the Al mole fraction resulting from the larger jitter (± 20 ms) when the shutter is operated in regimes 2 and 3 in the digital alloy technique, the minimum nonzero alloy percentage is simply

$$x_{\min 12} = \frac{R_{AlAs} T_{12}}{P}, \tag{4a}$$

in order to always operate in regime 1, and not stray into regimes 2 or 3, and

$$x_{\min 23} = \frac{R_{AlAs} T_{23}}{P}, \tag{4b}$$

in order to pulse the shutter in regimes 1 and 2, but to avoid regime 3 altogether. In the above equations, R_{AlAs} is the AlAs growth rate, P the superlattice period, and T_{12} and T_{23} are the shutter time constants defined in Eqs. (3). For $R_{AlAs} = 0.32\ \mu$m/h, and a period of 20 Å, $x_{\min 12}$ and $x_{\min 23}$ are, respectively, 0.8% and 0.09%. The percentage error in Al mole fraction at these limits are $\pm 6\%$ and $\pm 100\%$ for $x_{\min 12}$ and $x_{\min 23}$, respectively. These percentage error values are purely functions of the shutter time constants and jitter, and are ideally zero in the limit of no jitter.

Another source of deviation in Al flux from programmed values is flux transients caused by changes in the temperature of the surface of the charge in the MBE cell, upon shutter opening and closing. In our case, this can be gauged by differences in maximum Al flux values observed throughout the growth sequence and is $\leqslant \pm 0.12$ Å/s, translating to $\Delta x_{Al} \leqslant \pm 0.03$ at our growth conditions.

From the jitter in the profiles measured when the Al oven shutter is pulsed in the three regimes in the digital-alloy technique, one can estimate the percentage error in the Al mole fraction at various points in a symmetric parabolic well which has 0% Al in the well center. Two critical dimensions measured from the well center z_{C12} and z_{C23} can be defined. z_{C12} is the $\pm 6\%$ error point i.e., the distance from the well center where the Al mole fraction can vary by as much as $\pm 6\%$ of the design value, and this occurs when the shutter operation moves from regime 1 to 2; likewise z_{C23} is the $\pm 100\%$ error point, this occurring when the shutter operation moves from regime 2 to 3. For the particular Al oven shutter characterized above z_{C12} and z_{C23} are given, respectively, by

$$|z_{C12}| = \frac{L_{PW}}{2}\sqrt{\frac{x_{\min 12}}{x_{\max}}} \sim 325\ \text{Å}\left(\frac{L_{PW}}{4000\ \text{Å}}\right)\sqrt{\left(\frac{R_{AlGaAs}}{1\ \mu\text{m/h}}\right)\left(\frac{20\ \text{Å}}{P}\right)}, \tag{5a}$$

$$|z_{C23}| = \frac{L_{PW}}{2}\sqrt{\frac{x_{\min 23}}{x_{\max}}} \sim 110\ \text{Å}\left(\frac{L_{PW}}{4000\ \text{Å}}\right)\sqrt{\left(\frac{R_{AlGaAs}}{1\ \mu\text{m/h}}\right)\left(\frac{20\ \text{Å}}{P}\right)}, \tag{5b}$$

where $x_{\min 12}$ and $x_{\min 23}$ are as defined in Eqs. (4), $x_{\max}$ is the Al mole fraction at the well edges, P is the period of the superlattice grown, R_{AlGaAs} is the sum of the growth rates of GaAs and AlAs, and L_{PW} the width of the parabolic well. Similar critical dimensions for other alloy-profiles can also be derived. The percentage error in Al mole fraction will decrease approximately as z^{-2} for $|z| > z_{C12}$, is fixed at $\sim \pm 100\%$ for $|z| < z_{C23}$, and has values between $\pm 6\%$ and $\pm 100\%$ for values of z between the two critical z values. As stated earlier though, the problem can be avoided altogether by having a small nonzero minimum Al mole fraction $x_{\min 12}$ or $x_{\min 23}$ in the alloy.

The variation in the curvature of the parabolic well across a 2 in. diam wafer that is not rotated (to avoid interference between the frequency of rotation and the frequency of the shuttering in the digital-alloy case or of the temperature change in the analog-alloy case) is of interest. For the substrate/shutter/oven geometry for our Varian GEN II MBE machine we calculate a curvature variation of from $+30\%$ (at the point on the wafer farthest from the neighboring Al and Ga ovens) to -30% (at the point closest to the two ovens), 0% being at the wafer center, for both the digital and analog alloys. A further lateral nonuniformity is introduced in the digital-alloy case when the Al pulses become so sharp that the shutter only partially uncovers the oven thereby exposing the more distant points on the wafer to the Al flux for a longer time. This causes the curvature for $|z| < z_{C23}$ to vary from $+60\%$ (at the most distant point) to -100% (at the nearest point, which may not be receiving any Al flux at all) across the wafer, for our machine geometry and shutter time constants.

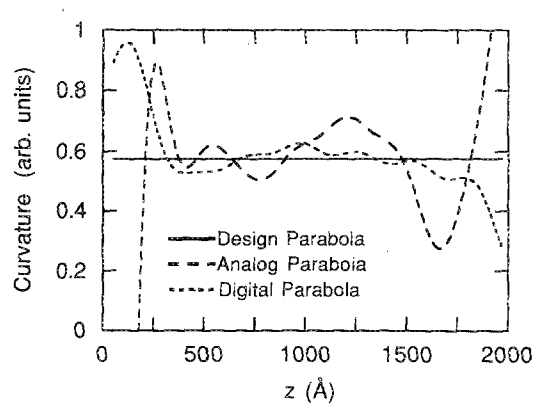

FIG. 7. Curvature vs depth of the three parabolic profiles: design, analog, and digital, shown in Fig. 4.

The ion gauge measured profiles are representative of the grown profiles only if both Ga and Al have unity sticking coefficient at the growth conditions. This is a function of substrate temperature, beam fluxes, etc.[13] At substrate temperatures above ~670 °C and As stabilized growth conditions, Ga re-evaporation will cause changes in both the layer thicknesses and the alloy composition, and therefore the alloy profile shape. An additional complication is that Ga re-evaporation is a function of the Al flux. Under such conditions, the graded-alloy profile is perhaps best measured by monitoring the desorbed Ga signal from the substrate during actual growth by a mass spectrometer mounted in one of the furnace ports with the analyzer having a line of sight view of the substrate.[14,15]

For our sample growth conditions (substrate temperatures of ~580 °C and As stabilized growth), the Ga and Al do have unity sticking coefficients. The growth rate of AlGaAs was measured by RED oscillations for a range of Ga and Al oven temperatures and was in all cases found to agree (within 1%) with the sum of the GaAs and AlAs growth rates, under the above growth conditions. The ion gauge measured profiles are therefore expected to be the actual alloy profiles grown.

This method can be used to calibrate the alloy grades of other ternary alloy films such as $In_xGa_{1-x}As$ and alloys with mixed group V elements such as $GaAs_xP_{1-x}$ and $GaSb_xAs_{1-x}$. If the InGaAs alloy were grown as a strained digital alloy on a GaAs substrate, then the effect of lattice-mismatch strain on cation incorporation rates[16] at the actual growth conditions, would have to be taken into account to deduce the grown alloy profile from the ion gauge measured profile. The measurements would also be valuable in the growth of strained graded alloys with critical composition requirements to avoid misfit dislocations.

For the alloys with the mixed group V elements, the composition of the alloy is controlled at low temperatures by limiting the amount of the element with the greater sticking coefficient and providing an excess of the more volatile species. For example, the smaller As (the preferentially incorporated element) flux supplied to the $GaAs_xP_{1-x}$ surface to which an excess P (the more volatile element) flux is also supplied, will control the alloy fraction x. The ion-gauge measurement could be therefore done with the less volatile of the two group V elements. The higher vapor pressure of group V elements might complicate the measurement though.

Since the currents measured are small (nA), the resolution of this measurement technique is ultimately limited by the resolution and speed of the picoammeter in this range. The overall accuracy of the actual graded alloy grown is still limited by the $\pm$ 3% accuracy of the measurement of GaAs and AlAs growth rates by the RED oscillation method.

III. CONCLUSIONS

In conclusion, we have presented a direct technique to measure graded $Al_xGa_{1-x}As$ alloy deposition profiles versus depth with a high degree of precision. The beam flux monitor ion gauge measured profiles are obtained in a dummy run immediately prior to actual growth in an MBE machine. Both a variable Al oven temperature technique (analog alloy) and a pulsed Al beam technique (digital alloy), have been applied to the case of a wide symmetric parabolic well. A computer is used to ramp the furnace temperature or pulse the beam with sufficient fineness to produce a smooth alloy grade, as evidenced by the corresponding ion-gauge measurements. The digital–alloy technique is further seen to be the preferable technique where changes in Al mole fraction versus depth are too rapid for the Al oven temperature to track precisely, and where reasonable growth rates are desired. Variations from run to run are small enough that one can use these measured profiles as a good indication of the actual graded Al mole fraction versus depth, grown.

The method is applicable to measuring the alloy grades of other III–V ternary alloys, especially where critical composition control is required to avoid misfit dislocations in the growth of strained graded alloys.

ACKNOWLEDGMENTS

We thank R. M. Westervelt, E. G. Gwinn, P. F. Hopkins, and A. J. Rimberg of Harvard University and P. O. Holtz, K. Ensslin, M. Sherwin, and P. Hillner of UCSB for valuable discussions. This work was supported in part by the AFOSR under Grant No. AFOSR-88-0099.

[1] W. T. Tsang, *Semiconductors and Semimetals*, edited by R. Dingle (Academic, New York, 1987), Vol. 24, Chap. 7.
[2] H. Kroemer, Proc. IEEE **70**, 13 (1982).
[3] F. Capasso, Chap. 6, *Semiconductors and Semimetals*, edited by R. Dingle (Academic, New York, 1987), Vol. 24, Chap 6.
[4] A. C. Gossard, J. Quant. Electronics QE **22**, 1649 (1986).
[5] M. Sundaram, A. C. Gossard, J. H. English, and R. M. Westervelt, J. Suplat. Microst. **4**, 683 (1988).
[6] M. Shayegan, T. Sajoto, M. Santos, and C. Silvestre, Appl. Phys. Lett. **53**, 791 (1988).
[7] E. G. Gwinn, R. M. Westervelt, P. F. Hopkins, A. J. Rimberg, M. Sundaram, and A. C. Gossard, Phys. Rev. B **39**, 6260 (1989).
[8] S. Adachi, J. Appl. Phys. **58**, R1 (1985).
[9] J. P. Harbison, L. D. Peterson, and J. Levkoff, J. Cryst. Growth **81**, 34 (1987).
[10] M. Kawabe, M. Kondo, N. Matsuura, and Kenya Yamamoto, Jpn. J. Appl. Phys. **22**, L64 (1983).
[11] R. C. Miller, A. C. Gossard, D. A. Kleinman, and O. Munteanu, Phys. Rev. B **29**, 3740 (1984).
[12] J. J. Harris, B. A. Joyce, and P. J. Dobson, Surf. Sci. **103**, L90 (1981).
[13] C. T. Foxon, J. Vac. Sci. Technol. B **4**, 867 (1986).
[14] A. J. Spring Thorpe and P. Mandeville, J. Vac. Sci. Technol. B **6**, 754 (1988).
[15] J. Y. Tsao, T. M. Brennan, J. F. Klem, and B. E. Hammons, Proceedings of the Ninth MBE Workshop, Purdue University, West Lafayette, IN, 1988 (unpublished).
[16] K. R. Evans, C. E. Stutz, D. K. Lorance, and R. L. Jones, J. Vac. Sci. Technol. B **7**, 259 (1989).